

---

# The $\gamma$ -ray burst of 980425 and its association with the extraordinary radio emission from a most unusual supernova

S. R. Kulkarni<sup>1</sup>, D. A. Frail<sup>2</sup>, M. H. Wieringa<sup>3</sup>, R. D. Ekers<sup>4</sup>, E. M. Sadler<sup>5</sup>,  
R. M. Wark<sup>3</sup>, J. L. Higdon<sup>3</sup>, E. S. Phinney<sup>6</sup>, and J. S. Bloom<sup>1</sup>

<sup>1</sup> Division of Physics, Mathematics & Astronomy, Caltech 105-24, Pasadena CA 91125, USA

<sup>2</sup> National Radio Astronomy Observatory, Socorro, NM, 87801, USA

<sup>3</sup> Paul Wild Observatory, Locked Bag 194, Narrabri NSW 2390, Australia

<sup>4</sup> Australia Telescope National Facility, CSIRO, P.O. Box 76, Epping, NSW 2121, Australia

<sup>5</sup> School of Physics, University of Sydney, NSW 2006, Australia

<sup>6</sup> Division of Physics, Mathematics & Astronomy, Caltech 130-33, Pasadena, CA 91125, USA

---

*This manuscript has been submitted to Nature on 29 June 1998. We are making this available via astro-ph given the intense interest in SN 1998bw and its relation to GRB 980425. You are free to refer to this paper in your own paper. However, we do place restrictions on any dissemination in the popular media. The article is under embargo until it is published. For further enquiries please contact Dale Frail (dfrail@nrao.edu) or Shri Kulkarni (srk@astro.caltech.edu).*

Supernova SN 1998bw exploded in the same direction and at about the same time as the gamma-ray burst GRB 980425. Here we report radio observations of this type Ic supernova, beginning 4 days after the gamma-ray burst. At its peak the radio source is the most luminous ever seen from a supernova,  $\nu L_\nu = 4 \times 10^{38} \text{ erg s}^{-1}$  at 5 GHz. More remarkably, the traditional synchrotron interpretation of the radio emission requires that the radio source be expanding at an apparent velocity of at least twice the speed of light, indicating that this supernova was accompanied by a shock wave moving at relativistic speed. The energy  $U_e$  associated with the radio-emitting relativistic electrons must lie between  $10^{49} \text{ erg} < U_e < 10^{52} \text{ erg}$ , and thus represents a significant fraction of the total kinetic energy  $\sim 10^{51} \text{ erg}$  associated with supernova explosions. The presence of a relativistic shock in SN 1998bw suggests a physical connection with the gamma-ray burst GRB 980425. We argue that this represents a second class of gamma-ray burst, with much lower emitted energy  $\sim 10^{48} \text{ erg}$  in gamma-rays than the two powerful  $\sim 10^{53} \text{ erg}$  high-redshift gamma-ray bursts previously identified.

It is only within the last year that we have begun to understand GRBs. At least one GRB is known to be securely of extragalactic origin<sup>1</sup> and the energy release,  $E_0$ , of another GRB has been estimated to be as high as  $10^{53} \text{ erg}$  (ref. 2). This revolution in our understanding is due to accurate localization of GRBs by the Italian-Dutch satellite BeppoSAX<sup>3</sup> and the discovery of relatively long-lived emission at X-ray<sup>4</sup>, optical<sup>5</sup> and radio wavelengths<sup>6</sup> – the so-called “afterglow” phenomenon. The burst itself and especially the afterglow emission are nicely accounted for by “fireball” models<sup>7,8,9</sup> which are similar to supernova models but with material (“ejecta”) moving at relativistic speeds. The inferred mass of the ejecta ( $M_{ej}$ ) is an astonishingly small  $10^{-5} M_\odot$ . Speculations for the cause of this explosion abound but most of them involve the formation of a black hole. In one set of models, the black hole is the end product of coalescence of neutron stars and in another model the black hole is the end product of a massive star. The reader is referred to refs. 10,11 for overviews.

Like GRBs, supernovae (SNe) are also explosive events, but are much more numerous. The observed light curves and spectra are used to classify supernovae and while it is not firmly established, astronomers believe that SNe of Type II, Ib and Ic mark the death of a massive star resulting in the formation of a neutron star or a black hole. SNe of type Ia are popularly attributed to the destruction of a massive white dwarf. The bulk of the observable energy is initially in the form of the kinetic energy of the ejected mass  $M_{ej}$ ,  $1M_\odot \lesssim M_{ej} \lesssim 20M_\odot$ . Estimates of the total kinetic energy  $E_0$  for SNe appear to cluster in a narrow range around  $10^{51} \text{ erg}$ . The ejecta move at speeds  $\sim \sqrt{2E_0/M_{ej}} \sim 10^9 \text{ cm s}^{-1}$  and the resulting shocks produce X-ray and optical emission.

Three parameters are sufficient to model the evolution of an astronomical explosion, be it SN or GRB: the kinetic energy released ( $E_0$ ), the mass (“ejecta”) in which this energy is initially deposited,  $M_{ej}$ , and the density of the ambient gas. The primary difference between SNe and GRBs lies in the the mass and hence in the speed and optical depth of the ejecta: high optical depth and non-relativistic speeds  $\beta c$  in SNe,  $\beta \lesssim 0.2$  or a bulk Lorentz factor,  $\Gamma \lesssim 1.02$ ; and low optical depth and relativistic speeds in GRBs with bulk Lorentz factor,  $\Gamma \sim 300$ . Here, following the standard convention,  $\Gamma \equiv (1 - \beta^2)^{-1/2}$ . This difference accounts for the efficient high energy emission of GRBs and the lower efficiency and lower energy (optical) emission of SNe. Secondly, while the total energy released is about the same in SNe and GRBs ( $E_T \sim 10^{53.5} \text{ erg}$ ), in normal SNe, 99% of that energy is carried off by neutrinos. And the high optical depth means that 99% of the remaining 1% is converted into kinetic energy during adiabatic expansion. At interstellar particle densities  $< 10 \text{ cm}^{-3}$ , only  $10^{-4}$  of  $E_T$  escapes in electromagnetic emission during the early months, the rest of the kinetic energy being radiated by the supernova remnant over the following  $\sim 10^6 \text{ y}$ .

In this paper we present radio observations of SN 1998bw (ref. 12), the analysis of which leads us to suggest that this SN is a link between some GRBs and supernovae. SN 1998bw appears to have exploded within the joint time and spatial error box of GRB 980425 (ref. 13). The low probability ( $10^{-4}$ ) of finding such a young supernova within the compact error circle<sup>13</sup> of the GRB suggests an association<sup>12</sup> between SN 1998bw and GRB 980425. As discussed in detail below, the radio emission from SN 1998bw has several unusual properties, including being the most luminous<sup>14</sup> radio supernova ever observed. These unique features further strengthen<sup>15</sup> the case for association. Inspired by this identification, other coincidences between Type Ib/Ic SNe and gamma-ray bursts have been noted<sup>16,17</sup>. Thus SN 1998bw may not be the only example of this potentially new class of GRBs.

The arguments listed above in favor of the GRB–SN association are compelling but fail to provide an observational clue as to how a SNe can generate a burst of gamma-rays. Theoretical models<sup>17</sup> have great difficulty generating a burst of gamma-rays. In this paper we show how a simple interpretation of the radio data forces us to conclude that SN 1998bw had a shock moving at relativistic speed, ahead of the low velocity ejecta which powers the optical light curve. If our interpretation is correct (and fortunately it is amenable to observational verification) then we have identified a specific phenomenon – a relativistic shock – which could potentially generate a burst of gamma-rays at early times in a SN.

### GRB 980425

Soffitta et al.<sup>13</sup> detected a gamma-ray burst of  $\sim 30$  seconds duration in the BeppoSAX Gamma-Ray Burst Monitor and the Wide Field Camera (WFC) on 1998 April 25.90915 UT. Follow-up observations of the 8-arcmin (radius) WFC error circle were made beginning on April 26.31 UT (ref. 18) and May 2.60 UT (ref. 19) with the BeppoSAX Narrow Field Instruments (NFI). Two previously unknown X-ray sources were found, one of which (1SAXJ1935.0–5248) remained steady between the two epochs. The other, 1SAXJ1935.3–5252, was detected at  $(2.4 \pm 0.5) \times 10^{-3}$  count  $s^{-1}$  (1.6–10 keV) during the first 27.7 hrs of the April 26 observation, but was not detected during the next 16.6 hrs. The  $3\text{-}\sigma$  upper limit was  $1.8 \times 10^{-3}$  count  $s^{-1}$ . Nor was it detected during the May 2 observation and the corresponding upper limit is  $1.5 \times 10^{-3}$  count  $s^{-1}$ .

Thus initial searches for optical and radio afterglow from the gamma-ray burst concentrated on the NFI position of this variable source 1SAXJ1935.3–5252 (see Figure 1). Galama et al.<sup>20</sup> and Bloom et al.<sup>21</sup> reported the absence of any transient optical source brighter than  $R < 21$  mag with changes larger than  $\pm 0.2$  mag.

We initiated our program of radio observations at the Compact Array (ATCA), an interferometric East-West array operated by the Australia Telescope National Facility. Observations began on April 28.73 in the 6-cm and the 3-cm bands. From the analysis of data of April 28 and April 29 we reported<sup>14</sup> the absence of any radio source in the NFI error circle of 1SAXJ1935.3–5252 with a  $3\text{-}\sigma$  upper limit of 0.3 mJy. Similarly, by averaging the datasets from the May 10 to June 22 monitoring effort, we can derive upper limits of 0.4, 0.2 and 0.4 mJy in the 20-cm, 6-cm, and 3-cm bands, respectively. This sensitivity would have been sufficient to have detected the radio emission seen from GRB 970508 (ref. 6) and the two recently detected radio afterglows, GRB 980329 (ref. 22) and GRB 980519 (ref. 23). However, to date, we have detected only three radio afterglows out of twelve well localized-bursts. Thus the failure to find a radio afterglow of this GRB is not alarming or constraining.

### SN 1998bw

Inside the larger 8-arcmin field-of-view of the WFC, but not coincident with either of the two NFI X-ray sources, Galama et al.<sup>24</sup> noted a  $R=15.7$  mag object located on the western spiral arm of the barred spiral galaxy ESO 184-G82. This bright object was not present in the Digitized Sky Survey, and, furthermore continued to brighten. Consequently, Galama et al. suggested that the source was a possible supernova (SN). Spectra taken by Lidman et al.<sup>25</sup> appeared to rule out a type-II or type-Ia supernova. Sadler et al.<sup>15</sup> pointed out its similarities to the pre-maximum spectrum of SN 1998bw with the type-Ib supernova 1983N, while Patat and Piemonte<sup>26</sup> noted that its helium lines were weak or absent, making it more like the spectra seen in type-Ic supernova. Given these observational developments, the Central Bureau for Astronomical Telegrams designated this object SN 1998bw. In Figure 1, we summarize the various localizations.

Galama et al.<sup>12</sup> present an optical (UBVRI) light curve for SN 1998bw. They find a peak absolute magnitude in the B band of  $-18.9$  magnitude and remark that it is unusually luminous for a type Ib/Ic supernova<sup>27</sup>. However, there is considerable scatter in the peak luminosity of Type Ib/Ic. Indeed, the type Ic SN 1992ar was a magnitude brighter<sup>28</sup> than SN 1998bw. On the other hand, as noted above, the optical spectrum of SN 1998bw is certainly unusual. Further unusual properties are the late-time spectrum, and indications of abnormally high-velocity gas. At twenty days past maximum light the optical spectrum has weaker-than-normal and broader-than-normal absorption lines<sup>29</sup>. R. A. Stathakis (pers. comm.) notes that ejection velocities measured from the blue wings of the Ca II line are as high as  $60,000$  km  $s^{-1}$  at the beginning of May and  $30,000$  km  $s^{-1}$  in mid-May, 1998.

From optical spectroscopic observations<sup>25,30</sup> the redshift to ESO 184-G82 is measured to be 0.0083 (heliocentric). The detection of narrow line absorption from sodium D lines<sup>29</sup> at the redshift of ESO 184-G82 shows that the SN is either in or behind ESO 184-G82. The distance to this galaxy, assuming a Hubble constant of  $65 \text{ km s}^{-1} \text{ Mpc}^{-1}$ , is 38 Mpc. The SN 1998bw, even at an assumed distance of 38 Mpc, is already ten times brighter than a typical Type Ib/Ic SN. Thus we argue that SN 1998bw is unlikely to be an unrelated background SN (ie. even more distant) but indeed is located within ESO 184-G82.

### Radio Observations of SN 1998bw

In the course of searching for radio emission from 1SAX J1935.3–5252 we noted<sup>31</sup> that the brightest radio source in the WFC error circle, J193503.3–525045 coincided with the supernova candidate of Galama et al. and that it too brightened considerably by May 5.6 UT. This strong early detection of a SNe motivated us to begin a radio monitoring program initially in the 6-cm (centre frequency, 4800 MHz) and the 3-cm (8640 MHz) bands at the position of the X-ray transient. From May 7 we also observed in the 20-cm (1384 MHz) and the 13-cm (2496 MHz) bands and shifted the field center 3' NW to the position of SN 1998bw. The results of this monitoring effort are summarized in Table 1 and Figures 2 and 3.

The flux in the 3-cm band and in the 6-cm band rise approximately linearly with time. The rapid rise enables us to empirically establish the epoch of the origin of the radio emission to better precision than that obtained from optical measurements<sup>12</sup>. As can be seen from Figure 2, this epoch is close ( $\pm 2$  days) to the time of the gamma-ray burst. This further strengthens the case for a physical association between the GRB and the SN. Given the near coincidence of the initiation of the radio emission and the time of the GRB we assume that the epoch of radio emission was the same as that of GRB 980425.

A long ATCA observation (9 hrs) was obtained on day 10. The 6-cm flux showed a smooth increase from 37 mJy to 41.6 mJy, consistent with the overall rising flux. At the same time the 3-cm flux increased from 46 mJy to 57 mJy but with considerable (20%) scatter. The scatter could be due to pointing errors, since SN 1998bw was located on the half-power response of the 3-cm primary beam for this observation. On day 12 we obtained 11 observations spread over 7 hrs with SN 1998bw at the field centre. The variations in the flux are no larger than 6% at 6 cm and 3% at 3-cm. The almost daily observations from day 12 to 22 with SN 1998bw at the field centre show a smooth change in flux density with day-to-day variations  $< 5\%$  (20-cm) and  $< 1\%$  (13-cm).

A single observation was also made on the night of 1998 May 7.7 UT, using the SCUBA bolometer array on the 15-m James Clark Maxwell Telescope (JCMT). Although SN 1998bw was observed at low elevation ( $< 17^\circ$ ) it was detected in the 2-mm band with a flux density of  $39 \pm 11$  mJy. At 1.35 mm the value is  $-21 \pm 32$  mJy. We note that the 2-mm data point was taken very close to the peak of the 6-cm and 3-cm emission.

The flux reaches a maximum on day 12 with flux densities,  $S(\nu)$  of 49 mJy (in the 3-cm band) and 45 mJy (6-cm band). The emission decays on a timescale similar to that of the rise-timescale. This rapid flux evolution is mirrored in the spectral index ( $\alpha$ ) plot (Figure 3) with the largest changes occurring in the first 20 days; here  $\alpha$  is the power law spectral index defined by the equation  $S(\nu) \propto \nu^\alpha$ . When the flux in the 6-cm band peaks, the spectral index from 20-cm to 6-cm is approximately 2.

After day 20, a new component of emission emerged. A broad maximum was reached at 3 cm (23 mJy) and 6 cm (30 mJy) on day 30. The 20-cm light curve rose  $\sim 0.5 \text{ mJy day}^{-1}$  from day 12, reached a peak (29 mJy) on day 45 and thereafter decayed. Beyond day 35 the 3-cm, 6-cm and 13-cm fluxes have begun a simple decay,  $\sim 0.5 \text{ mJy day}^{-1}$ . During this time the spectral index, as measured between pairs of adjacent wavelengths, is asymptotically converging to a value between  $-0.5$  to  $-1.0$  (Figure 3).

### Comparison of RSN 1998bw with other radio supernovae

Superficially the radio light curve in Figure 2 resembles other radio SNe (hereafter we will use the abbreviation RSN for radio SNe). However, there are significant differences. In order to make a proper comparison of this RSN with other RSNs, we now summarize the known properties of RSNs. The reader is referred to Weiler et al.<sup>32</sup> and Weiler & Sramek<sup>33</sup> for recent observational reviews and Chevalier<sup>34</sup> for a theoretical overview.

Radio emission is seen only from Type II or Type Ib/Ic SNe. While only five type Ib and Ic SNe have been studied in any detail, they all exhibit a more rapid radio flux density evolution than type-II SNe. At centimeter wavelengths the Ib/Ic RSNs peak some 10 to 40 days after the initial explosion, while type II

RSNe peak from 50 to 1000 days. Thus from radio observations alone we can ascertain that SN 1998bw is not a type II RSN but a type Ib/Ic RSN.

The 6-cm flux ( $S_6$ ) peaks on day 12 and the spectral luminosity,  $4\pi S_6 d^2$  is  $\sim 8 \times 10^{28} d_{38}^2 \text{ ergs s}^{-1} \text{ Hz}^{-1}$ ; here and below we assume that SN 1998bw is located in the galaxy ESO 184-G82 at a distance of  $38d_{38}$  Mpc. According to Weiler et al.<sup>35</sup> RSNe of type Ib and Ic are standard candles with peak 6-cm spectral luminosity around  $1.9 \times 10^{27} \text{ erg s}^{-1} \text{ Hz}^{-1}$  (Type Ib) and  $6.5 \times 10^{26} \text{ erg s}^{-1} \text{ Hz}^{-1}$  (Type Ic). We caution the reader that this conclusion is based on only five Type Ib/Ic radio SNe, and the data for some of these is quite sparse. Nonetheless, RSN 1998bw is more luminous than any previously studied RSNe including the powerful type II SN 1988Z (ref. 36; redshift,  $z = 0.022$ ) which achieved a peak 6-cm spectral luminosity of  $2 \times 10^{28} \text{ erg s}^{-1} \text{ Hz}^{-1}$  three years after the initial explosion.

On longer timescales, RSN 1998bw continues to follow a pattern different from that of other RSNe. As stated earlier around about day 20, a new component appears. This component peaks at 6-cm at about day 30 after which the peak moves to longer frequencies whilst maintaining approximately the same flux density. The component peaks at 20-cm on about day 45. This frequency-dependent evolution ensures that the spectral index is not constant across the cm-wave band as can be seen in Figure 3. In contrast, at late times, the radio emission from previously known RSNe decays monotonically at all frequencies. This broad-band decay is interpreted in terms of an expanding optically thin synchrotron emission source; the expansion leads to the overall decay and the optical thin condition ensures that the spectral index is constant during the expansion. By day 50, it is clear that the flux in the shortest two wave-bands (3-cm and 6-cm) are declining. The spectral index between these two bands is  $\sim -1$  and can be reasonably interpreted as the spectral index of the optically thin portion of the synchrotron spectrum. Our measured spectral index is comparable to those measured in type Ib/Ic RSNe but different from the  $-0.5$  to  $-0.7$  of Type II RSNe<sup>32,36</sup>. Again, this result emphasizes that RSN 1998bw is not a type II RSNe.

### Constraint on the size from variability

The expected angular size of the expanding radio photosphere  $\theta_S$  can be estimated by assuming that the radio photosphere expands at the same speed as that inferred from optical spectroscopy which we noted earlier<sup>29</sup> to be  $v_O \sim 6 \times 10^9 \text{ cm}$ . We obtain  $\theta_S = 0.91 t_d v_{60} d_{38}^{-1} \mu\text{arcsec}$  where  $v_{60}$  is the assumed velocity of expansion in units of  $60,000 \text{ km s}^{-1}$  and  $t_d$  is time since explosion in units of days. Thus the expected angular radius on day 10 is about  $9 \mu\text{arcsec}$ . This is sufficiently small that one expects to see deep modulation of the received signal on timescales of hours, due to scattering<sup>37,38,39</sup> of the radio waves by density irregularities in the diffuse ionized medium of our Galaxy.

For the purpose of theoretical modelling, the Galactic ionized medium can be conveniently approximated by a thin screen located at an effective distance of  $D \sim 0.5\text{--}1 \text{ kpc}$ . Scattering is considered to be in the “weak” regime when the Fresnel scale,  $r_F = \sqrt{\lambda D / 2\pi}$  is smaller than  $r_0$ , the spatial scale of the irregularities in the scattering screen; here  $\lambda$  is the wavelength of observations. In this regime, the intensity variations are modest and  $m$ , the modulation index (defined as the ratio of the rms of the intensity variations to the mean) is well below unity. When  $r_0 \ll r_F$ , the scattering is considered to be in the “strong” regime and the multitude of  $r_0$ -sized patches within a single Fresnel scale result in multi-path propagation. The result is deep intensity variations.

Both  $r_0$  and  $r_F$  are functions of the observing frequency. Instead of talking in terms of  $r_0$  and  $r_F$  it is more convenient to talk in terms of the transition frequency<sup>39</sup>,  $\nu_0$ . Observations at frequency ( $\nu$ ) above  $\nu_0$  are in the weak regime and observations at lower frequency suffer from strong scattering. Assuming typical interstellar medium parameters for this direction<sup>40</sup>,  $\nu_0$  is in the frequency range 3–7 GHz, a frequency range nicely straddled by our ATCA observations. The Fresnel angle,  $\theta_F \equiv r_F / D$  evaluated at the transition frequency of (say) 5 GHz is  $\theta_0 \sim 4 \mu\text{arcsec}$ ; here and below we have set  $D$  to 1 kpc.

Interstellar scattering allows us to constrain source size as long as the source smaller than one of three characteristic angular scales: (i) “weak”,  $\theta_W = \theta_0 (\nu_0 / \nu)^{1/2}$ , (ii) “refractive”,  $\theta_R = \theta_0 (\nu_0 / \nu)^{11/5}$  and (iii) “diffractive”,  $\theta_D = \theta_0 (\nu_0 / \nu)^{-6/5}$ . In Figure 4 we display the various regimes of interstellar scattering. We immediately note that diffractive scattering may have been important only at the earliest times. Unfortunately, during this time SN 1998bw was not located at the field center and antenna pointing errors likely dominate the observed variations. Outside these times we are in the weak scattering or refractive scattering regimes.

The expected modulation index and the timescale for the variability is given in refs. 38,39. On day 12 the 3-cm and 6 cm data showed less than 3% and 6%, respectively, over 7 hrs. Using an upper bound of three times the observed fractional variation we find that a lower bound on the velocity of expansion of the radio photosphere is 70,000-90,000 km s<sup>-1</sup>. However, better constraints come from the lack of variability at the low frequencies. This is best seen in Figure 4 in which we see the 20-cm and 13-cm lie squarely in the refractive regime. Beginning at day 12 the fluxes at 20-cm and 13-cm rise smoothly over the next 10 days. After subtracting the smooth rise we find the day-to-day variations of 5% at 20-cm and 1% at 13 cm (over a period of 7 days). The expected modulation index depends on the assumed  $\nu_o$ , however, as can be seen in Figure 4 the 13 cm and 20 cm datapoints nicely bracket the assumed uncertainty in  $\nu_o$ . The modulation index over this range is expected to be  $\sim 35\%$  (ref. 38). From the theory of refractive scintillation we infer the expansion of the radio photosphere to be  $\gg v_o$ , and place a lower limit of  $0.3c$ .

As a cross-check on these estimates we note that the radio afterglow of GRB 970508 which is located at a similar Galactic latitude exhibited strong variability at 8.46 and 4.86 GHz for at least three weeks, from which it was possible to infer its angular size and deduce the expansion of this cosmological GRB fireball (Frail et al. 1997). Thus the absence of any scintillation in J193503.3–525045 is due to the rapid angular expansion of this relatively nearby radio source.

### Modelling the radio light curves

Radio observations of supernovae have been interpreted in the framework of the “mini-shell” model<sup>34</sup>. The ejecta push a decelerating shock ahead of themselves into the circumstellar material. The shocked circumstellar material is then subject to Rayleigh-Taylor instability. This instability can drive turbulent motions which amplify magnetic fields and help Fermi-accelerate<sup>41</sup> particles to relativistic energies. Accelerated electrons gyrate in the newly amplified magnetic field and generate strong synchrotron emission.

The fact that the observed radio flux density drops at low frequency while the flux density of optically thin synchrotron radiation would continue to increase with decreasing frequency requires a frequency-dependent absorption mechanism. The two dominant mechanisms are free-free absorption by the surrounding circumstellar matter (assumed to be ionized by the SNe or the progenitor) and synchrotron self-absorption. Chevalier<sup>34</sup> concluded that the delayed turn-on of the lower-frequency radio emission is best explained by free-free absorption. Subsequently, much of the RSNe data have been modelled<sup>32,33</sup> in the context of the minishell and free-free absorption model.

However, Shklovskii<sup>42</sup> noting the fast turn-on of SN 1983N, a type Ib RSN, suggested that synchrotron self-absorption was the dominant absorption mechanism. Recently, Chevalier<sup>43</sup> has reconsidered this issue and concludes that both absorption mechanisms may be important but that synchrotron self-absorption cannot be ignored for type Ib/Ic RSNe. Kulkarni & Phinney<sup>44</sup> conclude that self-absorption is the dominant opacity in Type Ib/Ic RSNe. However, it is also equally clear that free-free absorption is manifestly important in Type II RSNe.

We now return to SN 1998bw. We noted earlier that the radio emission is composed of two emission components (Figure 2). The first component, on about day 10, peaks in the 3-cm band with a flux of 50 mJy. This component has all the features of a classical synchrotron self-absorbed spectrum. Specifically on day 10 we infer a peak frequency,  $\nu_p \sim 10$  GHz and associated peak flux  $S_p \sim 50$  mJy. It is well known that in a homogeneous source with a powerlaw electron spectrum, the self-absorbed synchrotron spectrum exhibits a  $\nu^{5/2}$  power law for frequency less than  $\nu_p$ . The observed spectral index of 2 between 20-cm and 3-cm of 2 (Table 1, Figure 3) is in acceptable agreement with this expectation. Having made the case for a synchrotron self-absorbed spectrum we now apply diagnostics of synchrotron theory to our data.

Kulkarni & Phinney<sup>44</sup> show that despite the complication of external absorption, brightness temperature ( $T_B$ ) limits can be used to draw robust conclusions from the light curves of RSNe ; here  $T_B$  is

$$T_B(\nu) = \left(\frac{c^2}{2k}\right) \left(\frac{S(\nu)}{\pi\theta_S^2}\right) \nu^{-2}. \quad (1)$$

The robustness is obtained from the well known result<sup>45,46</sup> that  $T_B$  of a source radiating via the incoherent synchrotron mechanism is limited to  $T_{\text{icc}} \lesssim 10^{12}$  K. The origin of this limiting  $T_B$  is the “inverse-Compton catastrophe”. When  $T_B$  exceeds  $T_{\text{icc}}$  multiple inverse Compton scattering of the synchrotron radio photons

to  $\gamma$ -ray/X-ray energies begins to rapidly dominate the luminosity. Limits on the X-ray to  $\gamma$ -ray flux or plausible total luminosities thus limit  $T_B$  to  $\lesssim T_{\text{icc}}$ .

For our application, the precise value of  $T_{\text{icc}}$  does matter and we now give an improved estimate of this. Assuming  $\alpha = -1$  and  $\nu_p = 5$  GHz, following Readhead<sup>47</sup>, we find that ratio of the inverse Compton ( $L_{\text{ic}}$ ) luminosity to the luminosity in synchrotron photons ( $L_{\text{synch}}$ ) is given by

$$\frac{L_{\text{ic}}}{L_{\text{synch}}} = \left(\frac{T_B}{4 \times 10^{11} \text{ K}}\right)^5 \left[1 + \left(\frac{T_B}{4 \times 10^{11} \text{ K}}\right)^5\right]. \quad (2)$$

From the BeppoSAX NFI X-ray observations on day 1 and day 8 we infer an upper limit ( $3\sigma$ ) on the 1.6–10 keV flux from the SNe,  $f_X < 10^{-13} \text{ erg cm}^{-2} \text{ s}^{-1}$ . On day 10, when the radio emission peaks in the cm-wave radio band, the 6-cm flux,  $S_R = 50 \text{ mJy}$  and thus the flux in the radio band is  $S_R \nu_R \sim 2.5 \times 10^{-15} \text{ erg cm}^{-2} \text{ s}^{-1}$ . The ratio of the X-ray luminosity (if any) to the radio luminosity is thus below 40 and using this value in Equation (2) we obtain  $T_{\text{icc}} \lesssim 5 \times 10^{11} \text{ K}$ . A more precise value depends on the cutoffs in the particle distribution and the  $T_B$  adopted, which set the location of the ‘‘Compton humps’’ in the spectrum.

Assuming that the angular radius of the source  $\theta_S = v_0 t/d$  where  $v_0 = 60,000 v_{60} \text{ km s}^{-1}$  is the assumed photospheric expansion speed and using Equation (1) the inferred brightness temperature is  $T_B = 2.0 \times 10^{13} S(\text{mJy})(\lambda/6 \text{ cm})^2 v_{60}^{-2} t_d^{-2} d_{38}^2 \text{ K}$ ; here  $S$  is the flux at wavelength  $\lambda$ . As can be seen in Figure 5, if  $v_0 = 60,000 \text{ km s}^{-1}$ , the inferred  $T_B$  greatly exceeds  $T_{\text{icc}}$  at all the observing frequencies.

Clearly, we have erred in one of our assumptions. What went wrong? As discussed earlier, the SNe cannot be in the foreground because of the interstellar absorption at the red-shift of the host galaxy ESO 184-G82, and if it is a background object the resulting  $T_B$  as well as the peak optical brightness would be even higher. The origin of the time for the radio emission is reasonably secure (to within a day or so) as can be seen from looking at Figure 2. Thus our assumed  $v_0$  must be incorrect.

### Relativistic Shocks

The preceding argument forces us to abandon the idea that the radio emitting region expands is coincident with the optical photosphere. Let the expansion speed of the radio emitting front be  $v = \beta c$ ; here  $v$  is the velocity of the expanding front and  $c$  the speed of light. Then the apparent transverse expansion angular speed is  $\Gamma \beta c$  where  $\Gamma = (1 - \beta^2)^{-1/2}$  is the Lorentz factor. For a source at distance  $d$  observed at time  $t$  after the explosion, the specific intensity  $I_\nu = (S/\pi)(d^2/(\Gamma \beta c t)^2) = 2kT_B \nu^2/c^2 = 2k\mathcal{D}T'_B(\nu')(\mathcal{D}\nu')^2/c^2$ . The last equality follows because  $I_\nu \nu^{-3}$  is a Lorentz invariant, and the Doppler factor  $\mathcal{D} = [\Gamma(1 - \beta \cos \theta)]^{-1}$  is of order  $\Gamma$  for the fastest moving material which dominates the emission. Thus the brightness temperature in the frame of the synchrotron-emitting plasma is

$$T'_B = 8 \times 10^{11} \Gamma^{-3} \beta^{-2} S(\text{mJy})(\lambda/6 \text{ cm})^2 t_d^{-2} d_{38}^2 \text{ K} \quad (3)$$

On day 4,  $S = 9.9 \text{ mJy}$  at 6-cm and from Equation (4) we obtain  $T'_B = 5 \times 10^{11} \text{ K}$ . If we insist that  $T'_B < T_{\text{icc}}$  then we obtain  $\Gamma^3 \beta^2 \gtrsim 1$ . Thus we conclude that the radio emitting region arises from a very fast moving shock,  $\Gamma > 1.4$  or  $\beta > 0.7$ . We now compute the total energy of this fast moving radio emitting shock. The energy is in the form of relativistic electrons ( $U_e$ ) and magnetic field strengths ( $U_B$ ); there could be a substantial amount of energy locked in protons but since protons do not radiate we cannot constrain this additional energy. It can be shown that  $U_B \propto S_p^{-4} \nu_p^{10} r^{11}$  and  $U_e \propto S_p^4 \nu_p^{-7} r^{-6}$  where  $r$  is the radius of the source. The total energy  $U = U_e + U_B$  thus depends sensitively on  $r$ . Furthermore, one term ( $U_B$ ) increases rapidly with  $r$  whereas the other ( $U_e$ ) decreases rapidly with  $r$ . Unfortunately, we have only a lower bound on  $r$ .

Scott & Readhead<sup>48</sup> were faced with same dilemma when investigating compact radio sources at meter wavelengths with ill-determined angular sizes. They noted that the total energy is minimized by a radius obtained by setting  $dU/dr = 0$ . This radius also results in equipartition of energy between the electrons and the magnetic field. Consequently, this radius is referred to as the ‘‘equipartition’’ radius,  $r_{eq}$  and the resulting total energy as the ‘‘equipartition’’ energy,  $U_{eq}$ . The equipartition angular radius,  $\theta_{eq} = r_{eq}/d$  is<sup>48</sup>

(note that many papers including ref. 48 define  $\theta_{eq}$  to be a diameter and  $S_\nu \propto \nu^{-\alpha}$ , while we define  $\theta_{eq}$  to be radius and  $S_\nu \propto \nu^\alpha$ )

$$\theta_{eq} = 120 \left( \frac{d}{\text{Mpc}} \right)^{-1/17} \left( \frac{S_p}{\text{mJy}} \right)^{8/17} \left( \frac{\nu_p}{\text{GHz}} \right)^{(-2\alpha-35)/34} \mu\text{arcsec} \quad (4)$$

It is convenient to express the total energy in terms of the equipartion energy,

$$\frac{U}{U_{eq}} = \frac{1}{2} \eta^{11} (1 + \eta^{-17}) \quad (5)$$

where  $\eta = \theta/\theta_{eq}$ .

On day 16  $\nu_p = 6$  GHz,  $S_p = 40$  mJy, so  $\theta_{eq} = 100 \mu\text{arcsec}$  ( $r = 6 \times 10^{16}$  cm at the distance of 38 Mpc),  $B \sim 0.4$  G, and  $U_{eq} = 10^{49}$  erg. Since  $r/t = 1.3c$ , this requires expansion of the radio photosphere at relativistic speed. This equipartition angular size corresponds to a brightness temperature  $T_B = 5 \times 10^{10}$  K, well below  $T_{icc}$ ; this  $T_b$  is nothing but the ‘‘equipartition’’ temperature ( $T_{eq}$ ) of Readhead<sup>47</sup>. The electrons radiating at  $\nu_p$  have energies of  $\sim 60$  MeV. If we had insisted on the size determined by the fastest optical lines ( $60,000 \text{ km s}^{-1}$ ), the radius would be 7 times smaller, and therefore the source energy would be dominated by relativistic electrons,  $U_e = 10^{54}$  erg —much larger than the total energy release in a supernova. Thus in addition to violating the X-ray constraint as discussed in the previous section, this low velocity solution is thus unacceptable on energetic grounds as well. This conclusion is robust since earlier we arrived at the same conclusion using an entirely independent method, viz. the lack of variability and interstellar scattering.

If we require only that the source not violate the X-ray inverse Compton constraint (Section 7), the brightness temperature could be ten times the equipartition value, the radius thus 1/3 the equipartition size (requiring  $v = 0.5c$ ), and  $U_e = 10^{52}$  erg. We thus conclude that, on day 16, the combined energy in the electrons and the magnetic field much lie in the range  $10^{49} \text{ erg} < U_e < 10^{52} \text{ erg}$ .

We can repeat this calculation for other dates. On days 4, 29 and 60, we adopt  $(\nu_p/\text{GHz}, S_p/\text{mJy}) = (10, 15), (3, 30)$  and  $(1, 20)$  respectively. These give  $\theta_{eq} = 35, 160, 400 \mu\text{arcsec}$ , and thus respectively  $r/t = 1.9c, 1.2c$  and  $1.5c$ .  $U_{eq} = 10^{48} \text{ erg}, 2 \times 10^{49} \text{ erg}$  and  $1.5 \times 10^{49} \text{ erg}$ . The angular sizes (and hence speeds) predicted above are verifiable with VLBI observations. The same observations will also directly yield the brightness temperature and thus the actual particle and field energies.

We close this discussion by noting some caveats.

- (i). *External Absorption.* We have ignored any possible external (i.e. free-free) absorption in our analysis. There will be some level of free-free absorption from ionized circumstellar material due to the progenitor star’s wind. It is clear from the asymptotic convergence of the band-to-band spectral indices to  $-1$  that least at late times there is little free-free absorption. However, we expect the circumstellar material to have a  $r^{-2}$  distribution and thus free-free absorption could well be important at early times. If so, the minimum energy and  $\Gamma$  deduced above are strict lower bounds.
- (ii). *Peak Frequency.* The highest inferred  $\Gamma$  comes from the earliest observations, day 4. Unfortunately, on that day we observed the source in only two bands. This limited coverage does not permit us to identify the true peak frequency. However, for a simple self-absorbed synchrotron source, one can quite easily demonstrate that inferring  $T_B$  or  $\theta_{eq}$  using flux measurement at a frequency other than  $\nu_p$  results in lower bounds on both quantities.
- (iii). *Expanding Synchrotron Source.* This, by far is the most serious concern. Our simple analysis was done under the framework of static synchrotron spheres. However, the radio photosphere is expanding at relativistic speeds. The portion expanding towards the observer becomes optically thin well before the back portion. Thus the observed spectrum will be more complex than that of a simple static synchrotron emitting sphere. Indeed, there is a suggestion that the broad-band spectrum on day 10 is not a pure synchrotron self-absorbed spectrum. The flux in the 2-mm band (JCMT observations) are well above a  $\nu^{-1}$  extrapolation. We are engaged in a detailed analysis of this problem.

## Geometry and Energetics

Above we concluded that the radio emission in RSN 1998bw arises in a shock with an initial  $\Gamma \gtrsim 2$ , which may have slowed to transrelativistic speed by the end of our observing period. The minimum total

energy in the radio-emitting region is  $\sim 10^{49}$  erg, a rather impressive energy considering the fact that most of the ejected mass is in a slower moving shock which manifests itself via the optical emission.

In the foregoing, we assumed spherical geometry. However, it could be that the radio emission is in the form of jets. This geometry has the advantage of reducing the energy requirements considerably. Fortunately, polarization measurements offer the possibility of probing the geometry of the emitting region. However, as can be noted from Table 1, we find no evidence for either circularly polarized signal or linearly polarized signal.

The circular polarization of synchrotron radiation from relativistic particles with a smooth pitch-angle distribution is small unless the radiation is close to the cyclotron limit. The absence of circular polarization is thus not surprising, though it does place a constraint on very slow jet models with magnetic fields well above equipartition.

Shear and expansion in non-spherical synchrotron sources like jets generally create magnetic fields with enough anisotropy that their integrated polarizations are high. For example the integrated fractional polarizations of radio quasars (including the core, the jet and the lobes) at 5 and 8 GHz are rarely below 4% (ref. 49), and bursts in BL Lac objects (believed to be caused by a single shock, as in the case of our supernova) have integrated linear polarizations  $\sim 10\%$ <sup>50,51</sup>. The lack of any linearly polarized signal could be reconciled with the jet hypothesis if the jet made an angle much greater than  $\Gamma^{-1}$  with respect to our line of sight. Because of aberration, we would then be seeing the back of the shock almost face-on, so a tangled field in the shock plane would produce no net polarization. However, this hypothesis would require that the intrinsic  $\Gamma$  and luminosity of the jet are much larger than the ones inferred above. This seems implausible.

The simplest interpretation of the observed low polarization is that we are seeing a spherical blast wave. A VLBI image could settle this uncertainty as well.

### A new type of GRB?

In our introduction we noted several circumstantial reasons favoring the association of GRB 980425 to SNe 1998bw. Clearly, if this association is correct then GRB 980425 is a new type of GRB, very different and much less energetic than the two GRBs at high redshift<sup>1,2</sup>. Differing in this conclusion are Wang & Wheeler<sup>16</sup> who suggest that all GRBs are associated with a SNe. In their model, the  $\gamma$ -ray emission has two components, a low-brightness isotropic component and a super-bright highly beamed component. They advocate that the  $\gamma$ -ray emission of GRB 980425 arises from the isotropic component and the gamma-ray emission from GRBs known to be at cosmological distances is due to the beamed component. We argue this hypothesis is incorrect. The afterglow, especially the very long-lived radio afterglow of cosmological GRBs such as that of GRB 970508 (ref. 6), is not subject to significant beaming. Nonetheless, the radio afterglow of GRB 970508 is far more energetic than the late time radio emission of SNe 1998bw. We conclude that if GRB 980425 is indeed associated with SNe 1998bw then it is a member of a new class of GRBs<sup>52</sup>.

Much theoretical effort<sup>11,7,8,9</sup> has been devoted to both the gamma-ray emission and the subsequent afterglow (which was indeed predicted before it was observed) of cosmological GRBs. The models give a reasonable description of the observed phenomena thereby boosting our confidence in them. The models posit that a large amount of energy  $E_0$  is mysteriously supplied to an astonishingly small mass of ejecta,  $M_{ej} \sim 10^{-5} M_\odot$ . The result is a very high- $\Gamma$  shock.

After day 4, the synchrotron lifetimes of the electrons in SN 1998bw radiating at  $\sim 5$  GHz are (for equipartition fields)  $\sim 1$  yr. [Note that the total energy radiated in the observed part of the radio spectrum is  $\sim 10^{45}$  erg, much less than  $U_{eq}$ . But the flat spectrum implied by the flux in the 2-mm band suggests that higher energy electrons may be more nearly radiative]. The X-ray flux limit implies that the inverse Compton losses cannot be much greater, so the shock appears to be non-radiative throughout the observing period. Extrapolating back in time in a simple equipartition model in which pressure  $p \propto r^{-2}$  and the particle spectrum is independent of radius, the optically thin synchrotron luminosity from radius  $r$  to  $2r$  scales as  $r^{-1}$ , as does the ratio of first inverse Compton to synchrotron luminosity. Thus at early times a shock in the circumstellar gas or an internal shock in the ejecta would be radiative and predominantly a gamma-ray source.

It is of some interest to note that more than two decades ago, Colgate<sup>53</sup> had proposed gamma-ray emission from SNe as possible origin of GRBs. The proposed mechanism, acceleration of the supernova shock to relativistic speed down the density gradient of a massive stellar envelope, has not been confirmed

by more detailed calculations including radiation coupling (e.g. ref. 54). Yet it might work with the much smaller and less massive envelopes of Carbon and Helium stars appropriate to type Ib/c supernovae. The gamma-ray burst energy is  $10^{48}$  erg which is smaller than the inferred minimum energy in the relativistic shock. Thus on energetic grounds, the relativistic shock can easily account for the observed gamma-rays. The outstanding theoretical issue now is how to generate a shock the required  $\Gamma$  and total energy, and avoid thermalizing the emitted spectrum.

Having established a physically motivated connection between SN 1998bw and GRB 980425 we now consider other such potential associations. In our view, the key factor which might make possible  $\gamma$ -ray bursts from SNe is the relativistic shock. At radio wavelengths, as argued extensively in this paper, the relativistic shock is manifested by high brightness temperature. Shklovskii<sup>42</sup> and later Slysh<sup>55</sup> noted that type Ib/Ic RSNe generally exhibit higher  $T_B$  than type II RSNe.

The earlier studies<sup>42,55,43</sup> noted the the possible presence of high velocity gas in type Ib/c RSNe. However, as reviewed elsewhere<sup>44</sup>, these earlier studies may have failed to appreciate how robust the arguments for high speeds were. If we insist that only a small portion of the SNe energy release should go into the radio-emitting shocks then we are forced to conclude that type Ib/Ic supernovae have shocks of at least transrelativistic speed.

As noted elsewhere<sup>44</sup>, the earliest measurements offer the greatest diagnostic of high- $\Gamma$  shocks. For example, for SN 1983N, the very first radio detection was 2 mJy in the 6-cm band (ref. 32). Following Chevalier<sup>43</sup>, the assumed epoch of this measurement is day 1 and a distance is 5.4 Mpc. The inferred  $T'_b \sim T_{eq}$ , requiring  $\Gamma^3 \beta^2 \gtrsim 1$  or  $\Gamma \gtrsim 1.3$ . Slysh<sup>55</sup> and Chevalier used later measurements and consequently missed the high speed shock. Unfortunately prompt radio observations of SNe are rare. Thus it is possible that relativistic shocks exist in other type Ib/Ic RSNe and were missed through lack of suitable observations.

We presented radio observations of SN 1998bw, a type Ic SN which has been associated with GRB 980425 on purely probabilistic grounds. This is the most luminous radio SN to date. Assuming that the radiation is synchrotron emission, we conclude that the shock in this SN must have a speed close to that of light, and a minimum energy  $\sim 10^{49}$  erg. This relativistic shock has apparent speed of  $2c$  on day 4, slowing down to  $c$  a month later. By analogy with GRBs we suggest that this relativistic shock could have generated a burst of gamma-rays at very early times. Thus our work provides a direct physical link between GRB 980425 and SN 1998bw. If this identification is correct, the variable NFI X-ray source 1SAXJ1935.3-5252 must have been an unrelated object, more likely to be a variable AGN than a true transient. It should therefore reappear in future X-ray observations.

As with any advance, there are many significant open questions. Is the shock spherical or collimated? How much energy beyond the minimum is involved in the relativistic shock? Is this phenomenon common to all Type Ic SNe? Fortunately, these questions can be answered by observations. Early time observations provide the best diagnostic of the fastest shock. VLBI observations could directly measure the geometry of the fast shock. And finally, it would be worth following up radio observations of GRBs with profiles similar to that of GRB 980425 (ref. 52).

**Acknowledgments.** We gratefully acknowledge Lorne Avery and Gerald Moriarty-Schieven for their help in making the JCMT observations. DAF thanks M. Rupen for useful discussions. SRK thanks A. Readhead for extensive discussions of brightness temperature. The Australia Telescope is funded by the Commonwealth of Australia for operation as a National Facility managed by CSIRO. The James Clerk Maxwell Telescope is operated by The Joint Astronomy Centre on behalf of the Particle Physics and Astronomy Research Council of the United Kingdom, the Netherlands Organization for Scientific Research, and the National Research Council of Canada. The VLA is a facility of the National Science Foundation operated under cooperative agreement by Associated Universities, Inc. The research of SRK and of ESP is supported by the National Science Foundation and NASA.

## References

1. Metzger, M. R. *et al.* Spectral constraints on the redshift of the optical counterpart to the gamma-ray burst of 8 May 1997. *Nature* **387**, 878-880 (1997).

2. Kulkarni, S. R. *et al.* Identification of a host galaxy at redshift  $z = 3.42$  for the  $\gamma$ -ray burst of December 1997. *Nature* **393**, 35-39 (1998).
3. Boella G. *et al.*, BeppoSAX, the wide band mission for x-ray astronomy. *Astron. Astrophys. Suppl. Ser.* **122**, 299-399 (1997).
4. Costa, E. *et al.* Discovery of an X-ray afterglow associated with the gamma-ray burst of 28 February 1997. *Nature* **387**, 783-785 (1997).
5. Van Paradijs, J. *et al.* Transient optical emission from the error box of the  $\gamma$ -ray burst of 28 February 1997. *Nature* **368**, 686-688 (1997).
6. Frail, D. A., Kulkarni, S. R., Nicastro, L., Feroci, M. & Taylor, G. B. The radio afterglow from the gamma-ray burst of 8 May 1997. *Nature* **389**, 261-263 (1997).
7. Mészáros, P. & Rees, M. J. Optical and long-wavelength afterglow from gamma-ray bursts. *Astrophys. J.* **476**, 232-237 (1997).
8. Vietri, M. The afterglow of gamma-ray bursts: the cases of GRB 970228 and GRB 970508. *Astrophys. J.* **488**, L105-L108 (1997).
9. Waxman, E. Gamma-ray-burst afterglow: supporting the cosmological fireball model, constraining parameters, and making prediction. *Astrophys. J.* **485**, L5-L8 (1997).
10. Fishman, G. J. & Meegan, C. A. Gamma-ray bursts. *Annu. Rev. Astron. Astrophys.* **33**, 415-458 (1995).
11. Piran, T. Towards understanding gamma-ray bursts. in *Unsolved problems in astrophysics*, Eds. J. N. Bahcall & J. P. Ostriker, Princeton University Press, 343-377 (1997).
12. Galama, T. J. *et al.* Discovery of the peculiar supernova 1998bw in the error box of GRB 980425. astro-ph/9806175, <http://xxx.lanl.gov> (1998).
13. Soffitta, P. *et al.* *Intl. Astron. Circ.* **6884**, (1998).
14. Wieringa, M., Frail, D. A., Kulkarni, S. R., Higdon, J. L. & Wark, R. *GCN Note No.* 63, (1998).
15. Sadler, E. M., Stathakis, R. A., Boyle, B. J., & Ekers, R. D. *Intl. Astron. Union* **6901**, (1998).
16. Wang, L. & Wheeler, J. C. The supernova-gamma-ray burst connection. <http://xxx.lanl.gov>, astro-ph/9806212 (1998).
17. Woosley, S. E., Eastman, R. G. & Schmidt, B. P. Gamma-ray bursts and Type Ic supernovae: SN 1998bw. <http://xxx.lanl.gov>, astro-ph/9806299 (1998).
18. Pian, E. *et al.* *GCN Note No.* 61 (1998a).
19. Pian, E., Frontera, F., Antonelli, L. A. & Piro, L. *GCN Note No.* 69 (1998b).
20. Galama, T. J. *et al.* *GCN Note No.* 62, (1998).
21. Bloom, J. S., Kulkarni, S. R., Djorgovski, S. G., McCarthy, P. & Frail, D. *GCN Note No.* 64, (1998).
22. Taylor, G. B, Frail, D. A., Kulkarni, S. R., & Shepherd, D. S. Discovery of the radio afterglow from the optically dim gamma-ray burst of March 29, 1998. *Astrophys. J.*, in press, (1998).
23. Frail, D. A., Taylor, G. B. & Kulkarni, S. R. *GCN Note No.* 89, (1998).
24. Galama, T. J., Vreeswijk, P. M., Pian, E., Frontera, F. Doublier, V. & Gonzalez, J. -F. *Intl. Astron. Union* **6895**, (1998).
25. Lidman, C. *et al.* *Intl. Astron. Union* **6895**, (1998).
26. Patat, F. & Piemonte, A. *Intl. Astron. Union* **6918**, (1998).
27. Miller, D. L., & Branch, D. Supernova absolute-magnitude distributions. *Astron. J.* **100**, 530-539 (1990).
28. Hamuy, M. *et al.* *Intl. Astron. Union Circ.* **5574**, (1992).
29. Stathakis, R. A. *et al.* Spectroscopy of SN 1998bw. in prep., (1998).
30. Tinney, C., Stathakis, R., Cannon, R. & Galama, T. *Intl. Astron. Union* **6896**, (1998).
31. Wieringa, M. *et al.* *Intl. Astron. Circ.* **6896**, (1998).
32. Weiler, K. W., Sramek, R. A., Panagia, N., van der Hulst, J. M., & Salvati, M. Radio Supernovae. *Astrophys. J.* **301**, 790-812 (1986).

33. Weiler, K. W. & Sramek, R. A. Supernovae and supernova-remnants. *Rev. Astron. Astrophys.* **26**, 295-341 (1988).
34. Chevalier, R. A. The radio and X-ray emission from type II supernovae. *Astrophys. J.* **259**, 302-310 (1982).
35. Weiler, K. W., van Dyk, S. D., Montes, M. J., Panagia, N., Sramek, R. A. Radio supernovae as distance indicators. *Astrophys. J.* in press, (1998).
36. van Dyk, S. D., Weiler, K. W., Sramek, R. A. & Panagai, N. SN 1988Z: the most distant radio supernova. *Astrophys. J.* **419**, L69-L72 (1993).
37. Narayan, R. The physics of pulsar scintillation. *Phil. Trans. R. Soc. Lond. A* **341**, 151-165 (1992).
38. Goodman, J. Radio scintillation of gamma-ray-burst afterglows. *New Astro.*, **2**, 449-460 (1997).
39. Walker, M. A. Interstellar scintillation of compact extra-galactic radio sources. *M.N.R.A.S.* **294**, 307-311 (1998).
40. Taylor, J.H. & Cordes, J.M. Pulsar distances and the galactic distribution of free electrons. *Astrophys. J.* **411**, 674-684 (1993).
41. Ball, L. & Kirk, J.G. The acceleration of electrons in the radio supernova SN 1986J. *Astron. Astrophys.* **303**, L57-L60 (1995).
42. Shklovskii, I. S. Synchrotron self-absorption of the radio emission of supernova 1983.51. *Sov. Astron. Lett.* **11**, 105-106 (1985).
43. Chevalier, R. A. Synchrotron self-absorption in radio supernovae. *Astrophys. J.* **499**, 810-819 (1998).
44. Kulkarni, S. R. & Phinney, E. S. Relativistic shocks in radio supernovae: Robust inference from brightness temperature. In preparation, (1998).
45. Hoyle, F., Burbidge, G.R., & Sargent, W.L.W. On the nature of the quasi-stellar sources. *Nature* **209** 751-753 (1966).
46. Kellerman, K. I. & Pauliny-Toth, I. I. K. The spectra of opaque radio sources. *Astrophys. J.* **155**, L71-L78 (1968).
47. Readhead, A. C. S. Equipartition brightness temperature and the inverse Compton catastrophe. *Astrophys. J.* **426**, 51-59 (1994).
48. Scott, M. A. & Readhead, A. C. S. The low-frequency structure of powerful radio sources and limits to departures from equipartition. *Mon. Not. Roy. Astr. Soc.* **180**, 539-550 (1977).
49. Conway, R.G., Haves, P., Kronberg, P.P., Stannard, D., Vallée, J.P., & Wardle, J.F.C. The radio polarization of quasars. *M.N.R.A.S.* **168**, 137-162 (1974).
50. Hughes, P.A., Aller, H.D. & Aller, M.F. Synchrotron emission from shocked relativistic jets. I. The theory of radio-wavelength variability and its relation to superluminal motion. *Astrophys. J.* **341**, 54-67 (1989).
51. Hughes, P.A., Aller, H.D. & Aller, M.F. Synchrotron emission from shocked relativistic jets. I. A model for the centimeter wave band quiescent and burst emission from BL Lacertae. *Astrophys. J.* **341**, 68-79 (1989).
52. Bloom, J. S. Kulkarni, S.R., Harrison, F., Prince, T., & Frail, D.A. Type Ib/Ic supernovae: A new class of gamma-ray bursts? in preparation, (1998).
53. Colgate, S. A. Early gamma rays from supernovae. *Astrophys. J.* **187**, 333-335 (1974).
54. Ensmann, L. & Burrows, A. Shock Breakout in SN 1987A. *Astrophys. J.* **393**, 742-755 (1992).
55. Slysh, V. I. Synchrotron self-absorption of radio emission from supernovae. *Sov. Astron. Lett.* **16**, 339-342 (1990).

**Table 1. Radio Flux Densities Measurements of SN 1998bw<sup>(a)</sup>**

Date (UT)	Elapsed Time (days)	S <sub>20</sub> (mJy)	S <sub>13</sub> (mJy)	S <sub>6</sub> (mJy)	S <sub>3</sub> (mJy)	Array Config.	Int Time (hrs)
1998 Apr 28	3.0			9.0	13.0	750A	3
1998 Apr 29	4.0			9.9	13.0	750A	2
1998 May 05	9.9			39.0	48.0	750A	9
1998 May 07	11.7	6.2	19.7	44.6	49.4	750A	3
1998 May 10	14.6	7.7	22.3	39.9	37.6	750A	2
1998 May 11	15.7	9.2	23.5	37.4	34.3	750A	2
1998 May 12	16.5	8.9	23.9	37.1	31.4	750A	1
1998 May 13	17.8	11.0	25.1	32.6	26.2	6C	3
1998 May 15	19.7	12.1	25.3	28.6	21.6	6C	0.5
1998 May 17	21.6	12.7	20.9	24.3	18.8	6C	1
1998 May 19	23.6	11.8	22.9	24.7	17.6	6C	1
1998 May 21	25.9	16.7	28.0	27.6	20.9	6C	0.5
1998 May 22	26.8	15.8	28.7	29.5	21.7	6C	0.7
1998 May 24	28.8	19.6	31.1	30.0	22.0	6C	1.3
1998 May 25	30.0	20.0	31.3	30.0	22.1	6C	2
1998 May 28	32.9	23.7	27.3	30.3	21.3	750E	1
1998 May 30	34.7	23.9	33.5	28.6	20.2	750E	1
1998 Jun 01	36.8	23.5	31.8	27.0	18.4	750E	1
1998 Jun 03	38.8	25.2	31.0	24.6	16.1	750E	0.8
1998 Jun 04	40.0	25.9	31.3	24.1	16.6	750E	0.6
1998 Jun 10	45.7	28.9	26.8	20.7	13.2	750E	1
1998 Jun 16	51.7	25.8	23.1	16.3	10.5	750E	2
1998 Jun 22	57.7	19.7	18.5	14.0	8.1	750E	2

(a) The entries (from left to right), the UT date of the observation, the time in days since the start of the SN explosion (calculated assuming that it occurred when the gamma-rays from GRB 980425 were first detected on 1998 March 25.90915 UT (ref. 13)), the flux density in milliJy at 20 cm (1.38 GHz), 13 cm (2.49 GHz), 6 cm (4.80 GHz), and 3 cm (8.64 GHz), the array configuration for the ATCA, and the total integration time obtained for each pair of wavelengths (20 cm/13 cm and 6 cm/3 cm).

(b) All observations used a bandwidth of 128 MHz and two orthogonal linear polarizations for each wavelength pair. The individual antenna elements were moved in the course of this monitoring effort, forming different array configurations (750A, 6C, 750E). We minimized the effects of confusion, an important issue for compact configurations such as 750A and 750E, by subtracting background sources from the visibilities, and by excluding the shortest baselines from the analysis.

(c) The initial pointing centre was toward 1SAX J1935.3–5252 but on 1998 May 07 it was shifted to SN 1998bw. All the tabulated flux density measurements of SN 1998bw prior to this date were corrected by the primary beam response of the antennas.

(d) A search was made for linear or circularly polarized flux on day 12. No signal was detected in the Stokes Q, U and V above 0.5% and 0.9% at 3 cm and 6 cm, respectively. The limits on day 29 and 30 are < 1.5% polarization at 3, 6 and 13 cm and < 2% linear polarization at 20 cm.

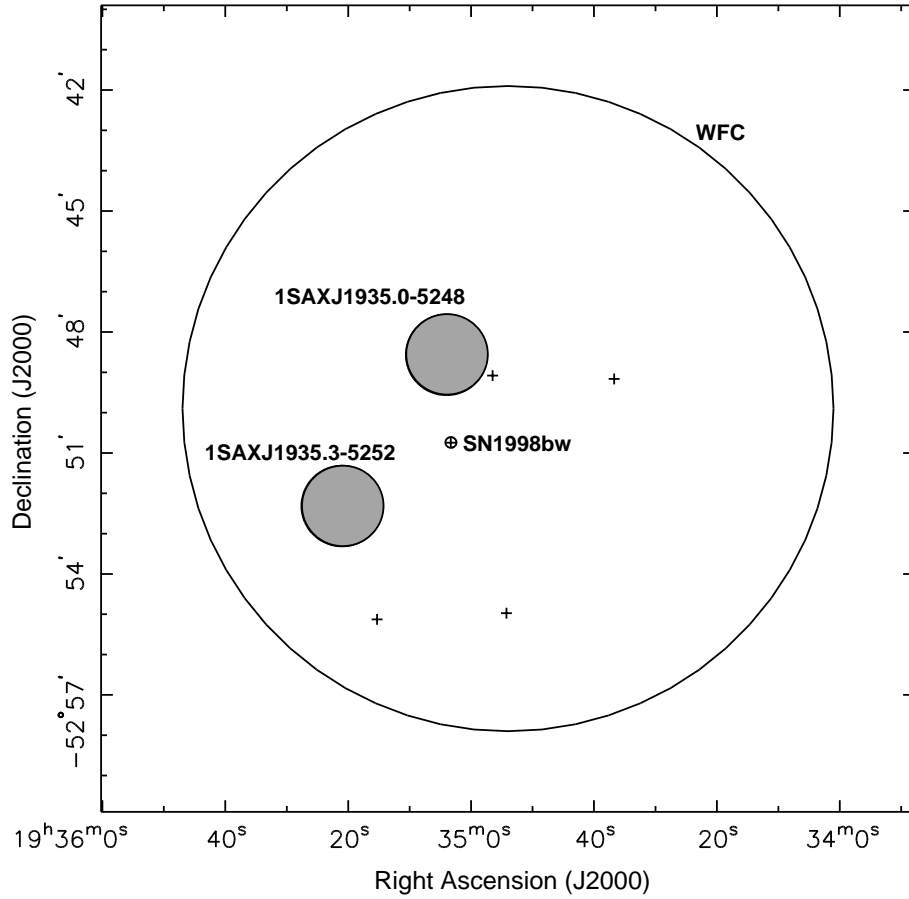
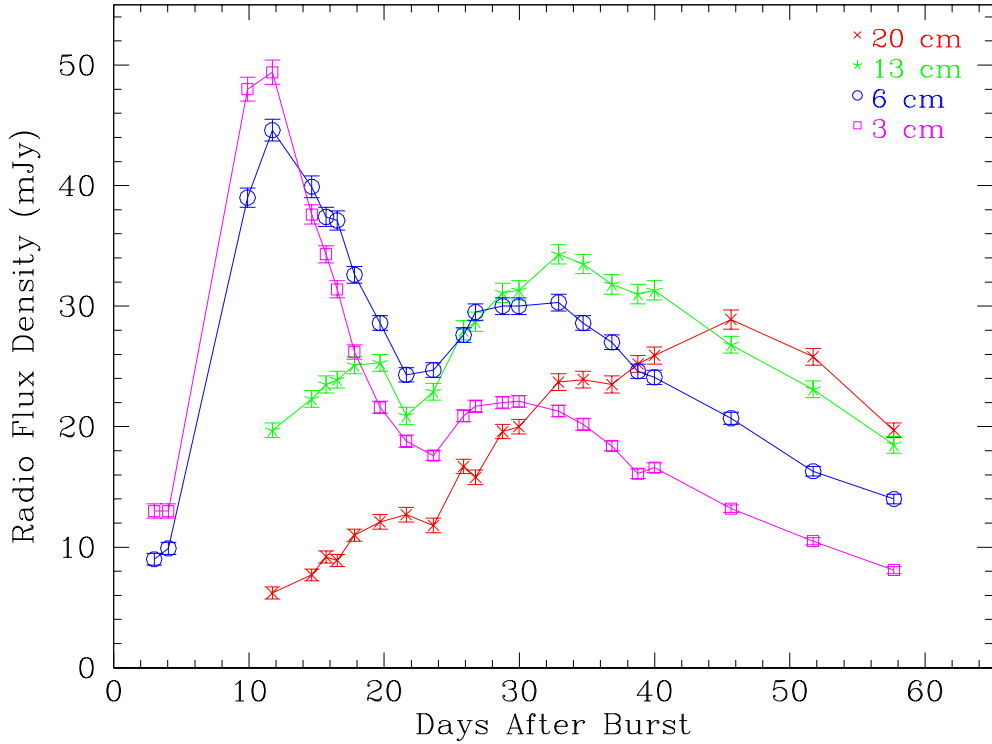
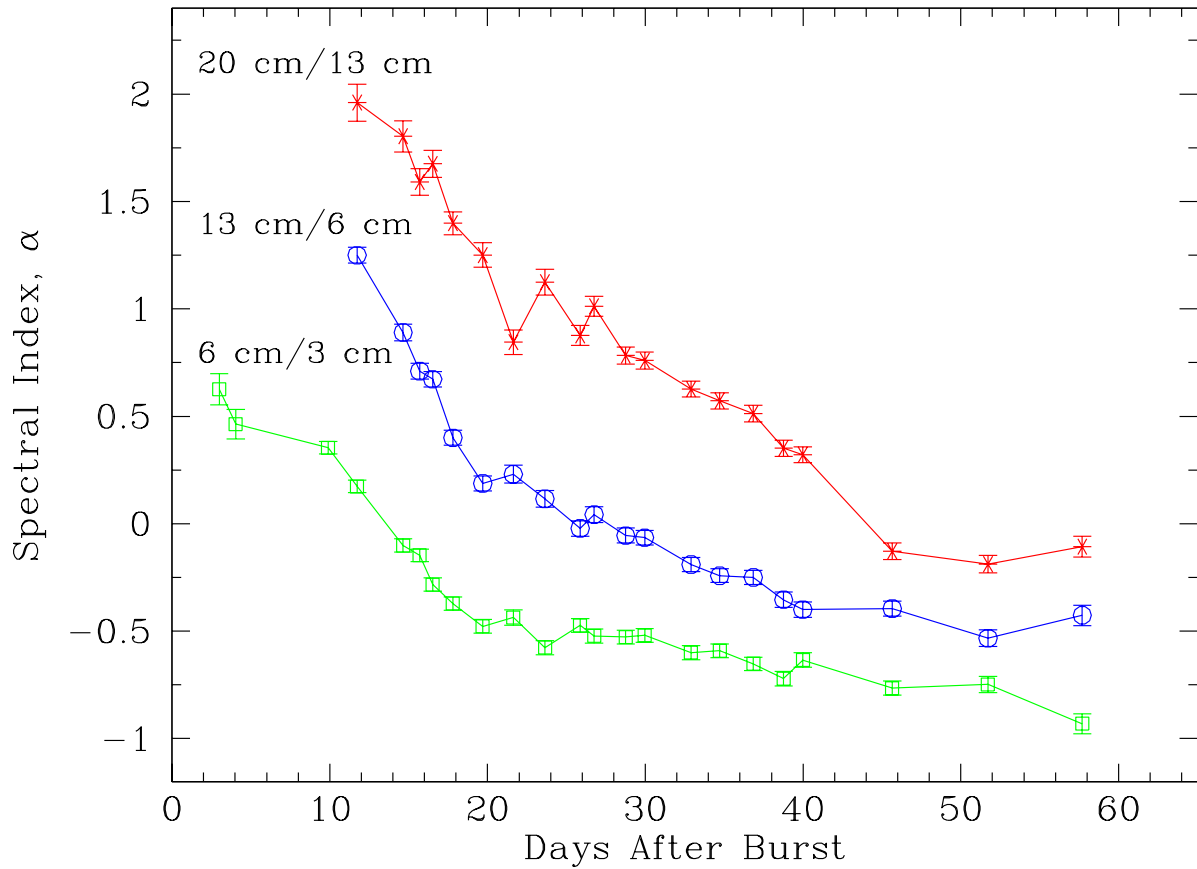


Figure 1. The position of objects within the 8-arcmin (radius) location error circle of the WFC for GRB 980425 (ref. 13). The two NFI X-rays sources<sup>18</sup> (the transient 1SAXJ1935.3–5252 and the steady 1SAXJ1935.0–5248) are indicated by hatched regions indicating their approximate position uncertainties. Small crosses indicate the positions of radio sources detected by the ATCA. The radio and optical emission from SN 1998bw is given by a circle with a cross. The mean position for SN 1998bw, obtained by averaging the best 3 cm and 6 cm observations, is  $\alpha = 19^{\text{h}}35^{\text{m}}3^{\text{s}}.316$  and  $\delta = -52^{\circ}50'44''.75$ , (equinox J2000). The  $1\text{-}\sigma$  error in  $\alpha$  is  $0^{\circ}.01$  and  $0''.07$  in  $\delta$ .



**Figure 2.**— The radio light curve of SN 1998bw. Four wavelengths, 20 cm (cross), 13 cm (star), 6 cm (circle) and 3 cm (square) are plotted together. The age of the supernova has been calculated assuming that the explosion date can be given by the detection of gamma-rays from GRB 980425. The error bars given on the plot are larger than the formal errors estimated from the receiver noise owing to the difficulties of determining the flux density with short snapshots. The errors, including absolute flux scale errors, thermal noise and confusion noise, can be approximated by the quadrature sum of a constant term (0.5 mJy for both 20 cm and 13 cm, 0.3 mJy for 6 cm and 0.2 mJy for 3 cm) and a term which is a fraction of the flux density (2%).



**Figure 3.**— The evolution of the radio spectral index for SN 1998bw. The spectral index  $\alpha$  (where  $S_\nu \propto \nu^\alpha$ ) is calculated between 20 cm and 13 cm (cross), 13 cm and 6 cm (open circle) and 6 cm and 3 cm (squares). The age of the supernova has been calculated assuming that the explosion date is given by the detection of gamma-rays from GRB 980425.

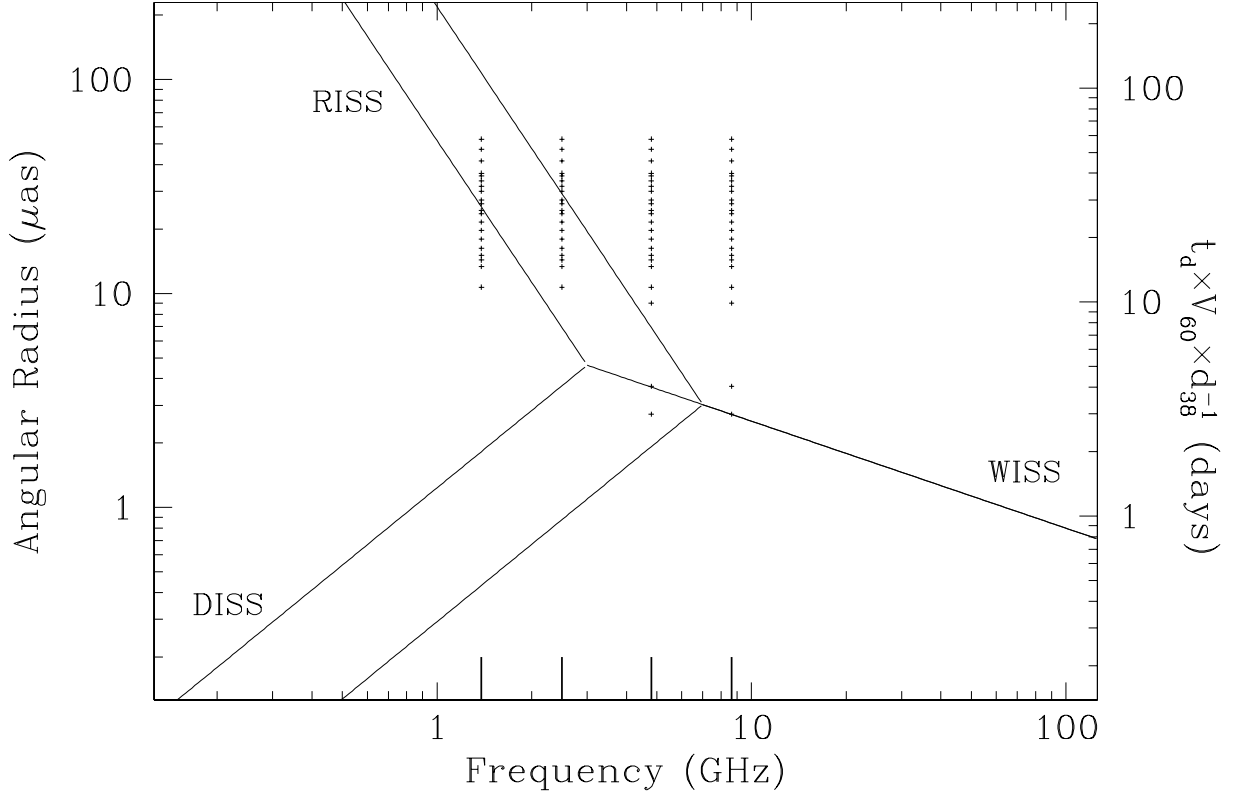


**Figure 4.**— The different regimes of interstellar scattering. Lines indicate the frequency dependence of diffractive (DISS), refractive (RISS) and weak (WISS) scattering as a function of the source angular radius (left hand axis). The exact value of the transition frequency between strong and weak scattering is uncertain ( $\nu_0=3\text{-}7$  GHz) and this is reflected in the plot by the different lines. On the right hand axis we plot the expected time (in days) that SN 1998bw would reach this radius if the velocity of the radio photosphere in units of  $60,000 \text{ km s}^{-1}$   $v_{60}=1$  and the source distance in units of 38 Mpc,  $d_{38}=1$ . Bold ticks at the bottom of the figure indicate the frequencies used in the ATCA observations. The small crosses are plotted at the frequencies and dates at which ATCA observations were made.

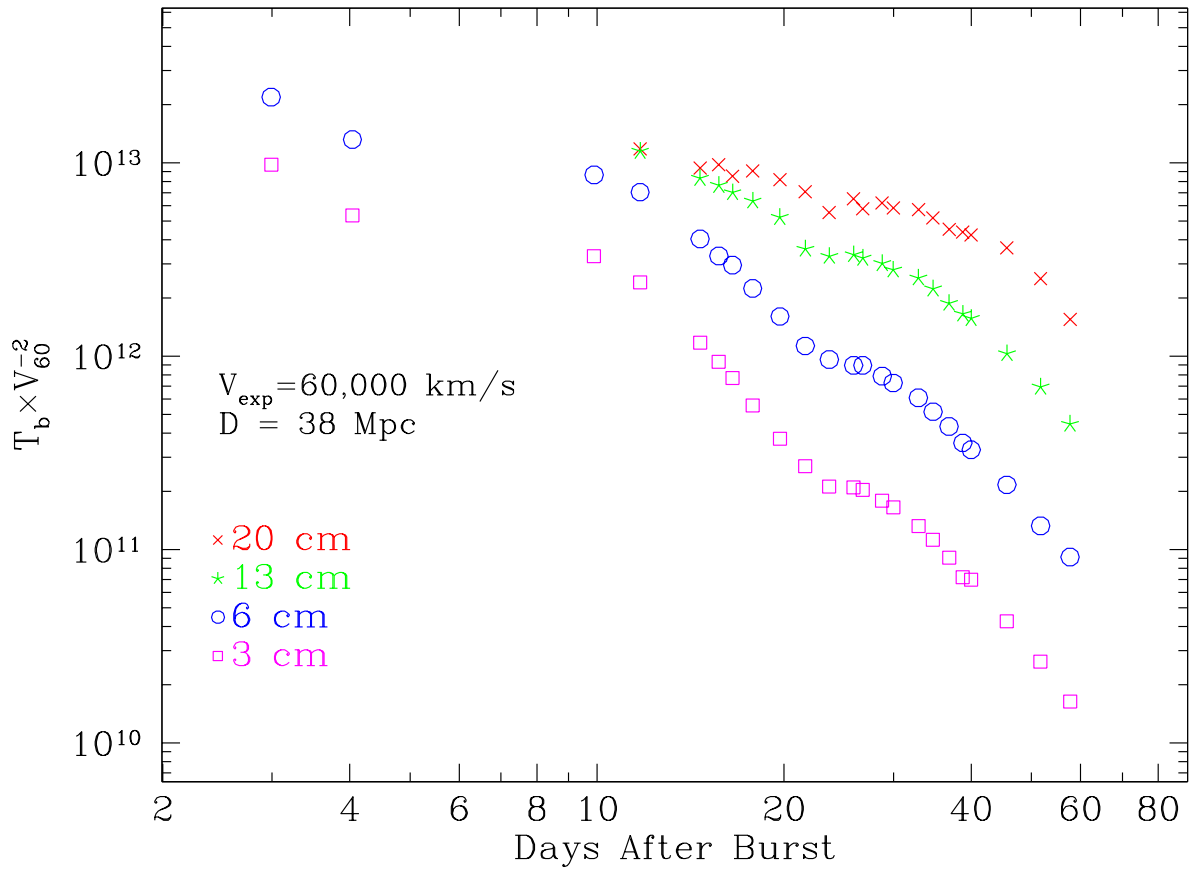


**Figure 5.**— The evolution of the brightness temperature of SN 1998bw at 20, 13, 6 and 3 cm. The y-axis is the brightness temperature assuming a distance of 38 Mpc and a velocity of  $v = 60,000v_{60} \text{ km s}^{-1}$ .